

# Synthesis and properties of carboxyl-substituted coumarin–phthalocyanine dyad dyes: effect of linker unit

Xuejun Zhang<sup>1</sup>  · Xilin Pei<sup>1</sup> ·  
Chaoqiang Liao<sup>1</sup> · Li Zou<sup>1</sup>

Received: 13 July 2016 / Accepted: 19 October 2016  
© Springer Science+Business Media Dordrecht 2016

**Abstract** Two novel coumarin-substituted phthalocyanine dyes (**CAPc** and **CSPc**) with different linking units, using carboxylic groups as electron acceptor and injector, were designed, synthesized, and applied as panchromatic organic sensitizers in  $I^-/I_3^-$ -based dye-sensitized solar cells (DSSCs). The asymmetric coumarin–phthalocyanine dyad analogue (**OAPc**) and the symmetric coumarin–phthalocyanine dyad analogue (**COPc**) were also synthesized for comparison. The structure–property relationship for these dyes was investigated by absorption spectroscopy, cyclic voltammetry, and thermogravimetric analysis. The ultraviolet–visible (UV–Vis) absorption was dramatically affected by the nature of the linker. Notably, modulation of the  $\pi$ -conjugated coumarin–phthalocyanine dyad **CAPc** and **CSPc** resulted in a large red-shift (Q-band above 710 nm); in particular, the dyad **CAPc** showed remarkably intense absorption in the spectral window of 450–650 nm. Electrochemical data for the dyes indicated that the azo double-bond-linked coumarin–phthalocyanine dyad dyes possessed relatively low-lying  $E_{\text{HOMO}}$  values, which may be beneficial to suppress electron back-transfer from the conduction band of  $\text{TiO}_2$  to oxidized dyes due to facile regeneration of the oxidized dye by the electrolyte. Thermogravimetric analysis showed that the three coumarin–phthalocyanine dyad sensitizers were stable above 200 °C. When the dyads were applied as light-harvesting sensitizers in dye-sensitized solar cells, the cell sensitized by **OAPc** showed the best power conversion efficiency of 2.4%.

**Keywords** Coumarin · Phthalocyanines · Linker · Absorption spectrum · Electrochemistry · Dye-sensitized solar cells

---

✉ Xuejun Zhang  
zhangxuejun@nuc.edu.cn

<sup>1</sup> College of Science, North University of China, Taiyuan 030051, Shanxi, China

## Introduction

Dye-sensitized solar cells (DSSCs) based on dye-sensitized nanocrystalline TiO<sub>2</sub> photoelectrodes with reduced manufacturing cost and facile processing have potential to compete with more mature photovoltaic solar cells based on Si in the future [1, 2]. Therefore, great efforts have been made to develop such low-cost solar cells over the last few years. Satisfactory conversion efficiencies have been achieved by using many organic or metalorganic molecules such as ruthenium [3, 4], coumarins [5, 6], porphyrins [7, 8], phenothiazine [9], phthalocyanines [10–12], and other small-molecule sensitizers [13–15]. The performance of DSSCs is mainly affected by the properties of the sensitizer [16], especially its absorption spectrum and energy levels.

Though organic dyes exhibit high molar extinction coefficient, they have narrow visible-range absorption spectra [17, 18]. To improve the light-harvesting potential of sensitizers, various notable attempts to achieve panchromatic absorption have been made, including: (1) cosensitization with multiple, complementarily absorbing dyes [8, 19], (2) integration of chromophores and auxiliary auxochrome (donors or acceptors) in one dye configuration [6, 11, 20], and (3) extending the conjugation structure of the dye molecule [6, 15, 17, 18]. On the other hand, intramolecular charge transfer from donor to acceptor has also been demonstrated to broaden the longer-wavelength absorption band to achieve panchromatic absorption and high photoelectron conversion efficiency [12, 21].

Phthalocyanines can serve as a near-infrared (IR)/IR motif in DSSC sensitizers owing to their intense absorption in the Q-band (around 700 nm) [10–12]. Furthermore, the intensity and region of light absorption by phthalocyanine derivatives can be enhanced and broadened by decorating the phthalocyanine core with complementary chromophores. Ren et al. [22, 23] reported phthalocyaninato zinc(II) substituted with tetrakis- or octabenzothiadiazole moieties, linked with alkynic bond or oxygen, achieving broad absorption covering the range of 300–900 nm. The superior red-shift and broadened absorption bands of these phthalocyanines arise due to their efficient conjugation structure and electronic interaction between the chromophores and phthalocyanine core. Yamamoto et al. [20] and Kc et al. [24] reported covalently linked Zn phthalocyanine–Zn porphyrin dyads with different linkages. These dyes combined the characteristic absorptions of the phthalocyanine and porphyrin.

Coumarin dyes are attractive due to their photoresponse at around 450 nm, excellent solubility, and fast electron injection [25]. When coumarin derivatives are introduced into a phthalocyanine core via a thioether bond, oxygen, alkoxy or phenoxy bridge, the absorption of the resulting coumarin-substituted phthalocyanine compounds between 450 and 600 nm is weak, despite the increased absorption range and solubility [26–29]. In previous study [30], we reported that integration of azobenzene on phthalocyanine was useful to increase the light-harvesting ability in the spectral window of 400–600 nm. As a result, dye-sensitized solar cells fabricated using such dyes including naphthalenyl showed improved efficiency compared with the dye including benzene. Also, the azobenzene branch provides the

opportunity to link other chromophores with various functional properties. Other research groups have demonstrated use of azobenzene or imino as an auxiliary chromophore, which was found to extend the absorption maximum and increase the molar extinction coefficient [30–33]. However, to the best of the authors' knowledge, coumarin–phthalocyanine dyad dyes covalently linked with oxygen, azo, or imino have not yet been reported for use in DSSCs. We believed that such covalently linked structures could be exploited for construction of coumarin–phthalocyanine dyads featuring this molecular configuration (Fig. 1). We varied the linker (oxygen, azo, and imino) to study its effects on the optical, aggregation, electrochemical, thermal, and photovoltaic properties.

## Experimental

### General methods

The scaffolds required to synthesize the target dyes, viz. 7-hydroxycoumarin-3-carboxylic acid, coumarin-3-carboxylic acid, 7-hydroxy-4-methylcoumarin, and 7-hydroxy-4-methylcoumarin-8-carbaldehyde, were obtained by Knoevenagel [28], Pechmann [34], and Duff [35] reactions according to literature procedures. 4-Methyl-7-(3,4-dicyanophenoxy)coumarin (**4**) was synthesized according to literature [26], then **COPc** was prepared according to literature method with minor modifications [27]. All other reagents were procured from commercial sources and used without purification. Solvents used for absorption spectrum and cyclic voltammetry measurements were distilled over suitable dehydrating agents according to standard methods. Column chromatography was performed with silica gel (**COPc**, **CAPc**, and **OAPc**) or activated alumina (**CSPc**).

Infrared (IR) spectra were recorded on a Shimadzu 4800S Fourier-transform infrared spectrophotometer in the range from 4000 to 450  $\text{cm}^{-1}$  from KBr pellets. The structures of the target compounds were confirmed by  $^1\text{H}$  nuclear magnetic resonance (NMR) spectra recorded on a Bruker AVANCE III 400-MHz spectrometer in dimethylsulfoxide ( $\text{DMSO}-d_6$ ), with chemical shifts reported relative to tetramethylsilane (TMS) as internal standard. Matrix-assisted laser desorption/ionization (MALDI) time-of-flight (TOF) mass-spectrometric measurements were performed on a Bruker Biflex III. Optical spectra in the UV–Vis region were

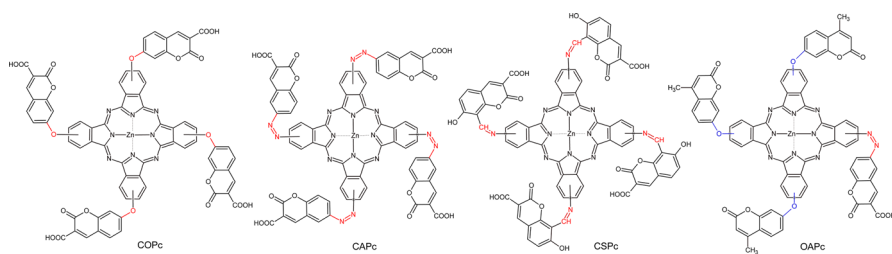


**Fig. 1** Structures of carboxyl coumarin–phthalocyanine dyad dyes

recorded on a Techcomp 2300 spectrophotometer using 1-cm-path-length cuvettes at room temperature. Different concentrations of dyes in solvent were obtained by stepwise dilution. Cyclic voltammetry measurements were carried out on an electrochemical workstation (VSP-300, Bio-Logic, France) using a three-electrode setup in which the working electrode and film counterelectrode were two platinum wires, with a standard calomel electrode (SCE) as reference electrode. The highest occupied molecular orbital (HOMO) and lowest unoccupied molecular orbital (LUMO) levels of the four coumarin-substituted phthalocyanine compounds were estimated using the following equations reported by de Leeuw et al. [36]:

$$E_{\text{HOMO}} = -(E_{\text{onset} \rightarrow \text{SCE}}^{\text{Oxy}} + 4.4 \text{ eV}),$$

$$E_{\text{LUMO}} = -(E_{\text{onset} \rightarrow \text{SCE}}^{\text{Red}} + 4.4 \text{ eV}).$$

Each dye was analyzed in dry dimethylformamide (DMF) containing tetrabutylammonium perchlorate (0.1 M) as supporting electrolyte. Before testing, nitrogen was inputted for 15 min to remove oxygen. Thermogravimetric analysis was carried out from 30 to 750 °C using a ZCT-A thermogravimetric analyzer in flowing nitrogen or flowing air (45 mL min<sup>-1</sup>) at heating rate of 10 °C min<sup>-1</sup>. The sample was prepared at 60 °C under vacuum for 12 h. Device fabrication followed a method similar to that reported recently [33]. Dye solutions were prepared at concentration of 1 × 10<sup>-6</sup> M in either THF or DMF containing 0.4 mM 3,7-dihydroxy-5*b*-cholic acid (CDCA). The electrolyte contained 0.05 M iodine and 0.5 M LiI in acetonitrile.

## Synthesis

### 7-(3,4-Dicyanophenoxy)coumarin-3-carboxylic acid (**1**)

A mixture of 1.73 g (10 mmol) 4-nitrophthalonitrile and 2.04 g (10 mmol) 7-hydroxycoumarin-3-carboxylic acid was dissolved in 35 mL DMF, and the solution was stirred and heated to 60 °C under nitrogen atmosphere. Subsequently, 4.1 g (30 mmol) fine anhydrous potassium carbonate was added in batches within 3 h and reacted for 32 h. Then, the reaction mass was poured into 120 mL ice water and the pH value adjusted to 4. The precipitate was filtered, and washed with water and ethanol several times until the filtrate became neutral, followed by recrystallization from a mixture of acetone/methanol (1:4 v/v) to obtain yellow-brown powder, which was finally dried under vacuum at 60 °C overnight. Yield: 67% (2.3 g). M.p.: 243–245 °C. Anal. Calc. for C<sub>18</sub>H<sub>8</sub>N<sub>2</sub>O<sub>5</sub>: C, 65.07; H, 2.43; N, 8.43. Found: C, 64.98; H, 2.44; N, 8.47. IR (KBr)  $\nu_{\text{max}}$ : 3146–2785 cm<sup>-1</sup> (COOH), 3075 cm<sup>-1</sup>, 3040 cm<sup>-1</sup> (C=C–H), 2234 cm<sup>-1</sup> (C≡N), 1708 cm<sup>-1</sup> (C=O), 1589, 1569, 1485 cm<sup>-1</sup> (C=C), 1310 cm<sup>-1</sup> (C–N), 1252 cm<sup>-1</sup> (Ar–O–Ar), 1202, 1093 cm<sup>-1</sup>. <sup>1</sup>H NMR (DMSO-*d*<sub>6</sub>, 400 MHz) ( $\delta$ , ppm): 10.73 (s, 1H, COOH), 8.53 (s, 1H, CH=C), 7.85 (d, 1H, Ar–H), 7.52 (s, 1H, Ar–H), 7.31 (d, 2H, Ar–H), 7.19 (d, 1H, Ar–H), 6.86 (s, 1H, Ar–H). MALDI-TOF MS calcd. for [M + H]<sup>+</sup> 333.27; found 333.18.

*6-(3,4-Dicyanophenylazo)coumarin-3-carboxylic acid (2)*

A mixture of 4-aminophthalonitrile (1.56 g, 11 mmol), concentrated hydrochloric acid (3 mL), and deionized water (30 mL) was stirred in an ice–water bath until thoroughly mixed. Then, a solution of sodium nitrite (0.76 g, 11 mmol) was added dropwise to the mixture during 20 min at approximately 0–5 °C, followed by constant stirring for another 40 min. Then, the reaction mixture was filtered, resulting in bright-yellow solution, which was kept at temperature around 0 °C for the next reaction. At the same time, coumarin-3-carboxylic acid (1.92 g, 10 mmol) was dissolved in 20 mL deionized water by adjusting the pH value to around 10 using sodium hydroxide solution (20%) in a three-necked flask. Then, previously prepared diazonium salt solution was added slowly to a stirred solution of coumarin-3-carboxylic acid as the coupling component in alkali medium with pH value controlled to around 9 while maintaining temperature of 0–5 °C. The resulting solution was stirred for 45 min in an ice–water bath, then removed to ambient temperature. Two hours later, dilute hydrochloric acid solution was added to adjust the pH value of the reaction solution to 5. The yellow–brown solid was filtered off, washed with ice water repeatedly, purified by recrystallization from methanol and acetone (1:1), and finally dried under vacuum at 40 °C overnight. Yield: 52% (1.79 g). M.p.: 178 °C. Anal. Calc. for  $C_{18}H_8N_4O_4$ : C, 62.75; H, 2.34; N, 16.27. Found: C, 62.70; H, 2.35; N, 16.32. IR (KBr)  $\nu_{\max}$ : 3137–2785  $cm^{-1}$  (COOH), 3073, 3038  $cm^{-1}$  (Ar, C–H), 2228  $cm^{-1}$  (C $\equiv$ N), 1732  $cm^{-1}$  (C=O), 1590  $cm^{-1}$  (Ar, C=C), 1490  $cm^{-1}$  (N=N), 1391  $cm^{-1}$  (C–N), 1374, 1316, 1249, 1132  $cm^{-1}$ .  $^1H$  NMR (DMSO- $d_6$ , 400 MHz) ( $\delta$ , ppm): 11.07 (s, 1H, COOH), 8.14 (s, 1H, CH=C), 7.93 (d, 1H, Ar–H), 7.81 (m, 2H, Ar–H), 7.68 (s, 1H, Ar–H), 7.60 (d, 1H, Ar–H), 7.36 (d, 2H, Ar–H). MALDI-TOF MS calcd. for  $[M + H]^+$  345.28; found 345.36.

*7-Hydroxy-8-(3,4-cyanophenylimino)coumarin-3-carboxylic acid (3)*

In a 250-mL three-necked flask, 1.17 g (5 mmol) 7-hydroxy-4-methylcoumarin-8-carbaldehyde and 1.14 g (8.5 mmol) anhydrous aluminum chloride were mixed, then 20 mL dichloromethane was added slowly until the aluminum chloride completely dissolved. Then, dichloromethane solution containing 1.73 g (10 mmol) 4-aminophthalonitrile and 3.5 mL (25 mmol) triethylamine was added dropwise to the reactor, with a lot of white mist; the colour of the mixture became red–brown. The solution was stirred at ambient temperature for 24 h. After completion of the reaction, 2.72 g (68 mmol, eight times that of  $Al_2O_3$ ) sodium hydroxide solution was added to the mixture. The white solid was filtered off, and the aqueous phase was extracted twice with dichloromethane. The organic layers were combined and dried over  $MgSO_4$ , and the solvent evaporated. The residue was purified by column chromatography on aluminum oxide using ethyl acetate/methanol (3:1) to obtain yellow powder. Yield: 37% (0.62 g). M.p. 209–212 °C. Anal. Calc. for  $C_{19}H_9N_3O_5$ : C, 63.51; H, 2.52; N, 11.70. Found: C, 63.47; H, 2.73; N, 11.68. IR (KBr)  $\nu_{\max}$ : 3172–2763  $cm^{-1}$  (OH), 3065, 3026  $cm^{-1}$  (Ar, C–H; N=C–H), 2227  $cm^{-1}$  (C $\equiv$ N), 1714  $cm^{-1}$  (C=O), 1682, 1632  $cm^{-1}$  (alkene, C=C, N=C), 1587, 1526, 1462,

1317  $\text{cm}^{-1}$  (C–N), 1254, 1108  $\text{cm}^{-1}$ .  $^1\text{H}$  NMR (DMSO- $d_6$ , 400 MHz) ( $\delta$ , ppm): 10.84 (s, 1H, COOH), 8.41 (s, 1H, CH=C), 8.26 (s, 1H, CH=N), 7.83 (m, 3H, Ar–H), 7.21 (d, 1H, Ar–H), 6.79 (d, 1H, Ar–H), 4.7 (s, 1H, OH). MALDI-TOF MS calcd. for  $[\text{M} + \text{H}]^+$  360.29; found 360.37.

*2(3),9(10),16(17),23(24)-Tetrakis(3-carboxycoumarin-7-oxy)phthalocyaninato zinc(II) (COPc)*

A mixture of **1** (0.67 g, 2 mmol), zinc acetate dihydrate (0.13 g, 0.6 mmol), and catalytic amount of 1,8-diazabicyclo[5.4.0]undec-7-ene (DBU) in *n*-pentanol (15 mL) was heated to 140 °C and stirred under nitrogen atmosphere for 24 h. After cooling to room temperature, the reaction mixture was precipitated by adding methanol (60 mL). The resulting black suspension was filtered off, and washed with deionized water and methanol. The black–green solid obtained after filtration was subjected to Soxhlet extraction using acetone for 24 h. Finally, the solid material was purified by silica gel column chromatography and eluted with trichloromethane, collecting a blue–green band. The product was obtained under reduced pressure. Yield: 37% (0.26 g). M.p. >300 °C. UV–Vis (DMF)  $\lambda_{\text{max}}$ : 345, 677 nm. Anal. Calc. for  $\text{C}_{72}\text{H}_{32}\text{N}_8\text{O}_{20}\text{Zn}$ : C, 61.98; H, 2.29; N, 8.03; found C, 61.89; H, 2.31; N, 8.06. IR (KBr)  $\nu_{\text{max}}$ : 3421  $\text{cm}^{-1}$  (COOH), 3031  $\text{cm}^{-1}$  (Ar–H), 1719  $\text{cm}^{-1}$  (C=O), 1607–1469  $\text{cm}^{-1}$  (Ar, C=C), 1233, 1101  $\text{cm}^{-1}$ .  $^1\text{H}$  NMR (DMSO- $d_6$ , 400 MHz) ( $\delta$ , ppm): 11.33 (s, 4H, OH), 8.65 (s, 4H, CH=C), 7.93–7.86 (m, 12 H, Pc–H), 7.51–7.23 (m, 12H, Ar–H,  $J = 8.0$  Hz). MALDI-TOF MS calcd. for  $[\text{M} + \text{H}]^+$  1395.47; found 1395.29.

*2(3),9(10),16(17),23(34)-Tetrakis(3-carboxycoumarin-7-azo)phthalocyaninato zinc(II) (CAPc)*

**CAPc** was synthesized following the procedure described above for **COPc**, except using 0.69 g (2 mmol) **2** instead of **1**. The solid material was purified using silica gel column chromatography and eluted with DMF:H<sub>2</sub>O:conc. HCl = 30:10:1 (v/v), collecting a black–green band. The product was obtained under reduced pressure. Yield: 0.67 g, 44%, M.p. >300 °C. UV–Vis (DMF)  $\lambda_{\text{max}}$ : 355, 553, 718 nm;  $^1\text{H}$  NMR (DMSO- $d_6$ , 400 MHz)  $\delta$ : 11.56 (s, 4H, COOH), 8.37 (s, 4H, coumarin unsaturation hydrogen CH=C), 8.18–8.29 (m, 12H, Pc–H), 8.12 (s, 4H, coumarin–H), 8.02–8.04 (d, 4H coumarin–H,  $J = 7.8$  Hz), 7.61–7.63 (d, 4H, coumarin–H,  $J = 8.8$  Hz); IR (KBr)  $\nu_{\text{max}}$ : 3407–3200  $\text{cm}^{-1}$  (carboxyl OH), 1715  $\text{cm}^{-1}$  (lactone, C=O), 1599–1491  $\text{cm}^{-1}$  (C=C), 1459  $\text{cm}^{-1}$  (N=N), 1095  $\text{cm}^{-1}$  (Ar–O–C). Anal. Calc. for  $\text{C}_{72}\text{H}_{32}\text{N}_{16}\text{O}_{16}\text{Zn}$ : C 59.89, H 2.22, N 15.53; found C 59.82, H 2.27, N 15.55. MALDI-TOF MS calcd. for  $[\text{M} + \text{H}]^+$  1443.53; found 1443.51.

*2(3),9(10),16(17),23(24)-Tetrakis(3-carboxycoumarin-7-imino)phthalocyaninato zinc(II) (CSPc)*

**CSPc** was synthesized following the procedure described above for **COPc**, except using 0.71 g (2 mmol) **3** instead of **1**. The solid material was purified by aluminum

oxide column chromatography and eluted with trichloromethane:methanol = 3:1 (v/v), collecting a gray–green band. The product was obtained under reduced pressure. Yield: 32% (0.24 g). M.p. >300 °C. UV–Vis (DMF)  $\lambda_{\text{max}}$ : 363, 716 nm. Anal. Calc. for  $\text{C}_{76}\text{H}_{36}\text{N}_{12}\text{O}_{20}\text{Zn}$ : C, 60.72; H, 3.42; N, 11.19; found: C, 60.67; H, 3.47; N, 11.07. IR (KBr)  $\nu_{\text{max}}$ : 3412, 3233  $\text{cm}^{-1}$  (O–H), 3024  $\text{cm}^{-1}$  (Ar–H), 1722  $\text{cm}^{-1}$  (C=O), 1604–1281  $\text{cm}^{-1}$  (Pc, C=N), 1265  $\text{cm}^{-1}$  (C–O–C), 1188, 1093, 1048  $\text{cm}^{-1}$ .  $^1\text{H}$  NMR (DMSO- $d_6$ , 400 MHz) ( $\delta$ , ppm): 11.47 (s, 4H, COOH), 8.43 (s, 4H, CH=N), 8.29 (s, 4H, CH=C), 8.07 (m, 12H, PcH), 7.84 (d, 4H, Ar–H,  $J = 8.0$  Hz), 7.25 (d, 4H, Ar–H,  $J = 8.0$  Hz), 5.21 (broad, 4H, OH) MALDI-TOF MS calcd. for  $[\text{M} + \text{H}]^+$  1503.57; found 1503.83.

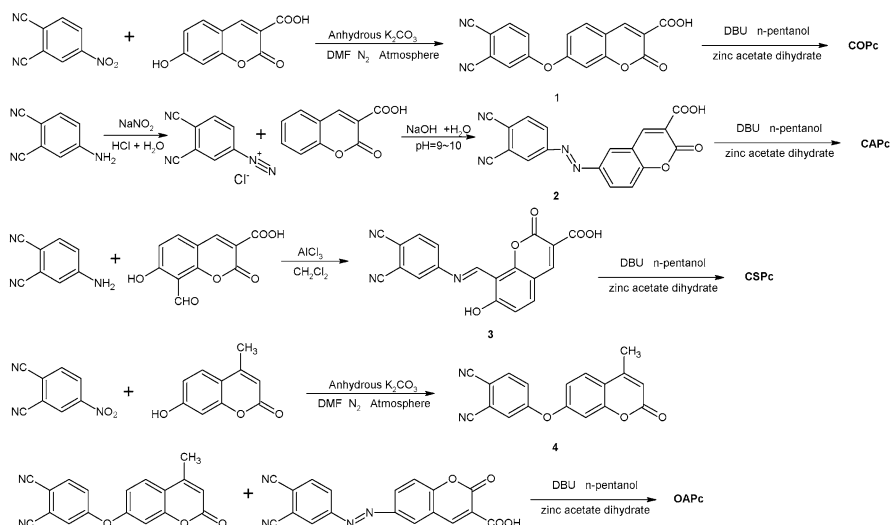
*2(3),9(10),16(17)-Tris(4-methylcoumarin-7-oxy)-23(24)-(3-carboxycoumarin-7-azo)phthalocyaninato zinc(II) (OAPc)*

**OAPc** was synthesized following the procedure described above for **COPc**, except using a mixture of 0.46 g (1.5 mmol) **4** and 0.17 g (0.5 mmol) **3** instead of **1**. The solid material was purified by silica gel column chromatography and eluted with DMF:THF = 1:3 (v/v), collecting a green band. The product was obtained under reduced pressure. Yield: 12% (0.16 g). M.p. >300 °C. UV–Vis (DMF)  $\lambda_{\text{max}}$ : 325, 500, 680 nm. Anal. Calc. for  $\text{C}_{72}\text{H}_{38}\text{N}_{10}\text{O}_{13}\text{Zn}$ : C, 65.65; H, 2.89; N, 10.64; found: C, 65.60; H, 3.01; N, 10.70. IR (KBr)  $\nu_{\text{max}}$ : 3394  $\text{cm}^{-1}$  (COOH), 3016  $\text{cm}^{-1}$  (Ar–H), 2948  $\text{cm}^{-1}$  ( $\text{CH}_3$ ), 1718  $\text{cm}^{-1}$  (C=O), 1643–1381  $\text{cm}^{-1}$  (Pc skeleton, C=C and N=N), 1236, 1091  $\text{cm}^{-1}$ .  $^1\text{H}$  NMR (DMSO- $d_6$ , 400 MHz) ( $\delta$ , ppm): 11.38 (s, 1H, COOH), 8.24 (s, 1H, CH=C), 7.17–7.32 (m, 30H, 12PcH, 6ArH), 7.13 (m, 6H, Ar–H,  $J = 8.4$  Hz), 6.39 (s, 3H, CH=C), 2.17 (s, 9H,  $\text{CH}_3$ ). MALDI-TOF MS calcd. for  $[\text{M} + \text{H}]^+$  1317.54; found 1317.49.

## Results and discussion

### Synthesis and characterization

Coumarin–phthalocyanine dyad dyes were synthesized following the protocol illustrated in Scheme 1. Alkylation of 4-nitrophthalonitrile with 7-hydroxycoumarin-3-carboxylic acid or 7-hydroxy-4-methylcoumarin in presence of  $\text{K}_2\text{CO}_3$  in DMF was performed to obtain coumarin-substituted phthalonitrile precursors 7-(3,4-dicyanophenoxy)-coumarin-3-carboxylic acid (**1**) and 4-methyl-7-(3,4-dicyanophenoxy)coumarin (**4**) [29, 32], respectively. Meanwhile, 4-aminophthalonitrile was subjected to diazo coupling [30] or Schiff-base condensation [37] reaction with coumarin-3-carboxylic acid or 7-hydroxy-4-methylcoumarin-8-carbaldehyde to obtain the required coumarin-substituted phthalonitrile precursors 6-(3,4-dicyanophenylazo)coumarin-3-carboxylic acid (**2**) and 7-hydroxy-8-(3,4-cyanophenylimino)coumarin-3-carboxylic acid (**3**). In the final step, the precursors **1**, **2**, **3** were condensed with zinc acetate by cyclotetramerization to produce the target coumarin–phthalocyanine dyad dyes 2(3),9(10),16(17),23(24)-tetrakis(3-carboxycoumarin-7-oxy)phthalocyaninato zinc(II) (**COPc**), 2(3),9(10),16(17),



**Scheme 1** Synthesis of carboxyl coumarin-phthalocyanine dyad dyes

23(34)-tetrakis(3-carboxycoumarin-7-azo)phthalocyaninato zinc(II) (**CAPc**), and 2(3),9(10),16(17),23(24)-tetrakis(3-carboxycoumarin-7-imino)phthalocyaninato zinc(II) (**CSPc**), respectively. The target dyad dye 2(3),9(10),16(17)-tris(4-methylcoumarin-7-oxy)-23(24)-(3-carboxycoumarin-7-azo)phthalocyaninato zinc(II) (**OAPc**) was obtained by reaction of 4-methyl-7-(3,4-dicyanophenoxy)coumarin (**4**) with 6-(3,4-dicyanophenylazo)coumarin-3-carboxylic acid (**2**). The dyad dyes were soluble in dimethyl formamide, dimethylsulfoxide, and pyridine, and sparingly in trichloromethane, tetrahydrofuran, triethylamine, etc. Finally, all intermediates and final targets were thoroughly analyzed by IR spectroscopy,  $^1H$  NMR, elemental analysis, and mass spectroscopy.

In the IR spectra, formation of compounds **1**, **2**, **3**, **4** was clearly confirmed by  $C\equiv N$  vibration at around 2230, 2234, 2228, and 2227  $cm^{-1}$ ,  $\alpha,\beta$ -unsaturated  $C=C$  of lactone ring at 1569  $cm^{-1}$ , and ether group  $C-O$  at 1208  $cm^{-1}$ , without vibrations of  $NO_2$  or  $NH_2$ . After conversion of the dinitrile derivatives **1**, **2**, **3**, **4** into the phthalocyanines **COPc**, **CAPc**, **CSPc**, **OAPc**, the sharp peak of  $C\equiv N$  vibration at around 2223  $cm^{-1}$  disappeared. The data are consistent with the proposed molecular structures. In addition, the  $^1H$  NMR and elemental analysis results were consistent with the proposed molecular structures; For example, the expected signals of **CAPc** in the  $^1H$  NMR spectra were observed in accordance with the proposed structure. Isomeric multiplet peaks located at 8.30–8.18 ppm with 12 protons were found for the Pc ring, making the calculation of coupling constants inaccurate. Aromatic protons of coumarin were observed as two sets of doublets at 8.04–8.02 and 7.63–7.61 ppm, integrating to eight protons. Three singlets located at 11.56, 8.37, and 8.12 ppm appeared, being ascribed to carboxyl acid protons, unsaturated protons, and coumarin C-5 protons, respectively, all of them indicating

four protons. The signal of carboxyl proton was observed to be broader and weaker due to its exchange with solvent.

### Absorption properties and aggregation behavior

The UV–Vis absorption spectra of the four dyes in DMF solution, exhibiting two types of characteristic absorption bands (Q-band and Soret band), are displayed in Fig. 2; the corresponding absorption data are listed in Table 1. The longer-wavelength stronger Q-band absorption band at 650–750 nm is lacking due to phthalocyanine ring  $\pi \rightarrow \pi^*$  transitions ( $a_{1u} \rightarrow e_g^*$ ) [38], whereas the shorter-wavelength broader Soret absorption band at 330–400 nm corresponds to transitions from  $a_{2u}$  and  $b_{1u}$  to  $e_g^*$  orbitals [37]. This result suggests that the optical properties of the phthalocyanine dyes can be finely tuned by altering the nature of the asymmetric structure. Using the equation  $E_{0-0} = 1240/\lambda_{\max}$ , the  $E_{0-0}$  energy for **COPc**, **CAPc**, **CSPc**, and **OAPc** was estimated to be 1.83, 1.73, 1.73, and 1.80 eV, respectively. The decrease of the energy gap of the dyad dyes results in a red-shift of the absorption band. The Soret bands of all the dyad dyes were broadened due to superimposition of phthalocyanine and coumarin in the  $\sim 450$  nm region, suggesting the absence of strong electronic interaction between the Pc and coumarin components in the ground state, resulting in an intramolecular color match. Meanwhile, the Q-band absorption ( $\lambda_{\max}$ ) of **OAPc** showed a slight red-shift (10 nm) or significant blue-shift (31 nm) compared with **COPc** and **CAPc**, respectively. On changing the linkage between coumarin and phthalocyanine, the diazo- and imino-conjugated coumarin–phthalocyanine dyad dyes **CAPc** and **CSPc** displayed broadened and red-shifted absorption at 718 and 715 nm compared with **COPc**, respectively. This can be explained by the fact that efficient incorporation of the coumarin ring and phthalocyanine core in the conjugation pathway increased the electron delocalization scope over the molecule, thus reducing the bandgap of the

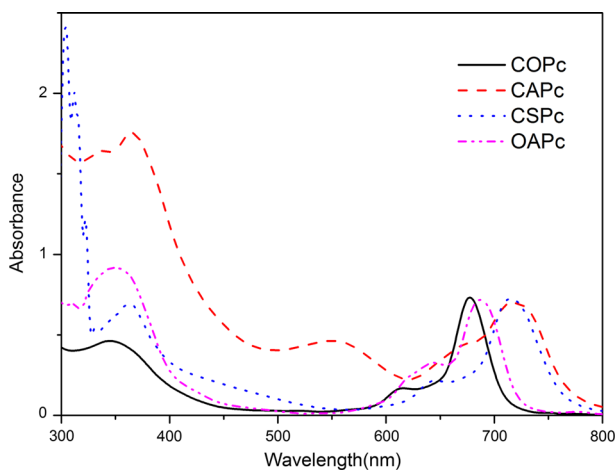


**Fig. 2** Absorption spectra for dyes **COPc**, **CAPc**, **CSPc**, and **OAPc** recorded in DMF

**Table 1** Electrochemical properties of **COPc**, **CAPc**, **CSPc**, and **OAPc**

Dyad	$\lambda_{\text{abs}}/\text{nm}$ ( $\epsilon_{\text{max}} \times 10^5 \text{ M}^{-1} \text{ cm}^{-1}$ )	$E_{\text{g}}^{\text{opt}}/\text{eV}$	$E_{\text{Onset}}^{\text{Oxy}}/\text{V}$	$E_{\text{HOMO}}/\text{eV}$	$E_{\text{LUMO}}/\text{eV}$
<b>COPc</b>	677 (2.47), 615 (0.56), 344 (1.60)	1.83	0.51	-4.91	-3.08
<b>CAPc</b>	718 (2.32), 551 (1.77), 358 (8.24)	1.73	0.77	-5.17	-3.44
<b>CSPc</b>	715 (2.42), 646 (0.71), 365 (2.29)	1.73	0.67	-5.07	-3.34
<b>OAPc</b>	777 (0.57), 687 (2.39), 644 (1.08), 350 (3.07)	1.80	0.71	-5.11	-3.31

dye. Interestingly, **CAPc** exhibited a new absorption in the range of 519–592 nm compared with **COPc** featuring oxygen linkage, and **CSPc** displayed intense absorption at around 400–550 nm. This is probably due to electron transfer from the peripheral, tetraazo substituent  $\pi^*$  orbital to the Pc 1s level [39]. This clearly indicates that the azo linker is a better choice than oxygen or imino regarding realization of panchromatic light harvesting.

It is also interesting to compare the aggregation behavior of the dyad dyes with oxygen, azo, and imino linkage, which helps to reveal the impact of the linker segment on the absorption profile.  $\pi$ - $\pi^*$  interactions between the  $\pi$ -electron clouds surrounding Pc macrocycles result in aggregation of phthalocyanine molecules [40]. In the aggregated state, the electronic structure of the complex phthalocyanine rings is perturbed, resulting in alteration of the ground- and excited-state electronic structures, leading to change of the molecular extinction coefficient and position of the Q-band [38]. In this study, the molar absorption coefficient of the stronger Q-band ( $\lambda_{\text{max}} = 677, 718, 715,$  and  $687 \text{ nm}$  for **COPc**, **CAPc**, **CSPc**, and **OAPc**, respectively) was monitored in the concentration range from  $1 \times 10^{-6}$  to  $8 \times 10^{-6} \text{ mol L}^{-1}$  in DMF to provide support for the change in aggregated species (Fig. 3). With increasing concentration, the absorption intensity of the Q-band maxima increased, the Beer–Lambert law was obeyed, and there was no blue-shift typical of aggregated species for **COPc**, **CSPc**, and **OAPc**, suggesting that the effects of the coumarin substituent on the phthalocyanine core prevented aggregation [41]. Interestingly, the intensity of the Q-band absorption for **CAPc** also increased, while the Beer–Lambert law was not obeyed as the concentration was increased. Furthermore, there was a more obvious change of the Soret band than the Q-band. The different bridge linkages in **COPc**, **CAPc**, and **CSPc** resulted in different aggregation behavior, which is ascribed to the double-azo bond being more rigid than the oxygen or imino bond [42], resulting in a more rigid structure that hinders the coumarin substitution compared with the other linker units.

### Electrochemical characteristics

To investigate the effect of the coumarin substituent on the electrochemical characteristics of the synthesized dyes as well as the feasibility of electron injection from the excited dye into the conduction band of  $\text{TiO}_2$  and dye regeneration from  $\text{I}^-/\text{I}_3^-$  redox electrolyte, the relative energy levels  $E_{\text{HOMO}}$  and  $E_{\text{LUMO}}$  are required.

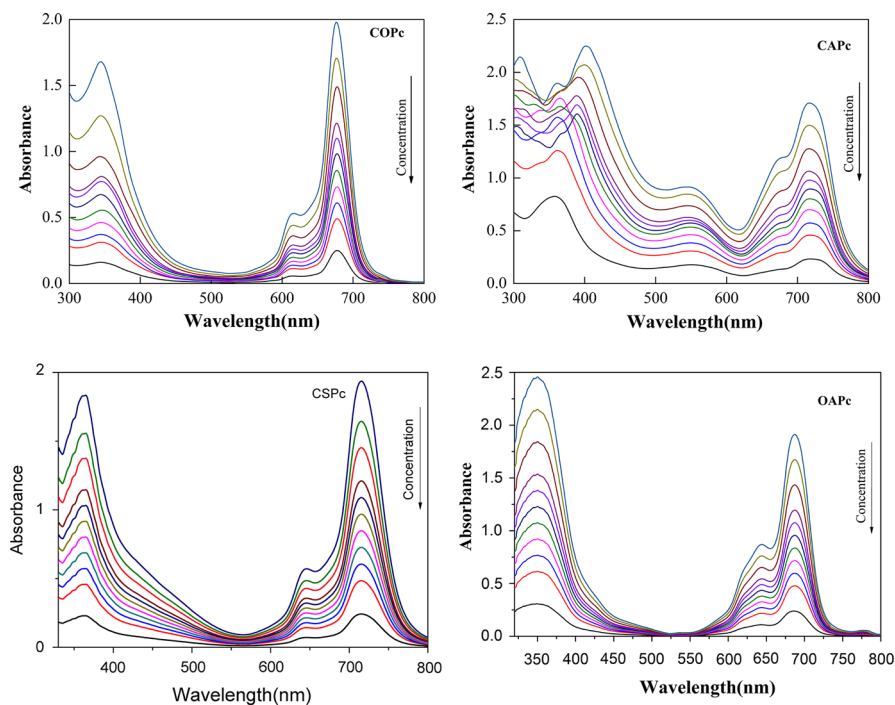


**Fig. 3** Absorption spectra for **COPc**, **CAPc**, **CSPc**, and **OAPc** dyes at different concentrations

To obtain these values, cyclic voltammograms were obtained in DMF at scan rate of  $100 \text{ mV s}^{-1}$  (Fig. 4); the corresponding data are presented in Table 1. In our experiment, it was found that all of the dyad dyes showed one quasireversible reduction couple, ascribed to reduction of four coumarin moieties, and a one-electron irreversible oxidation wave, attributed to oxidation of the Pc core. The oxidation onset potentials  $E_{\text{onset} \rightarrow \text{SCE}}^{\text{ox}}$  determined from the intersection of two tangents drawn at the rising current and baseline charging current of the cyclic voltammograms [13] for the dyes revealed the order: **COPc** (0.51 V) < **CSPc** (0.67 V) < **OAPc** (0.71 V) < **CAPc** (0.77 V). There are various interesting points, irrespective of the phthalocyanine core and coumarin substituent: the  $\pi$ -conjugated linked dyad dyes **CAPc** and **CSPc** showed higher oxidation potential than the oxygen  $p$ -conjugated linked dyad dye **COPc**. This clearly indicates that electron of  $\pi$ -conjugated dyes is more efficient than  $p$ -conjugated delocalization at the coumarin and phthalocyanine moieties. Also, for the asymmetric coumarin-substituted phthalocyanine **OAPc**, the coumarinazo moieties of the molecule facilitate oxidation, while the triscoumarinoxy moieties showed the opposite trend.

The  $E_{\text{LUMO}}$  level of the sensitizer corresponding to the excited-state oxidation potential is closely related to the electron injection efficiency of the  $\text{TiO}_2$  surface, and a higher  $E_{\text{LUMO}}$  level is helpful for providing higher electron injection potential [9, 21]. In general, the low  $E_{\text{HOMO}}$  level of the dye sensitizers corresponding to the oxidation onset potentials matches with the energy level of the  $\text{I}^-/\text{I}_3^-$  redox couple to

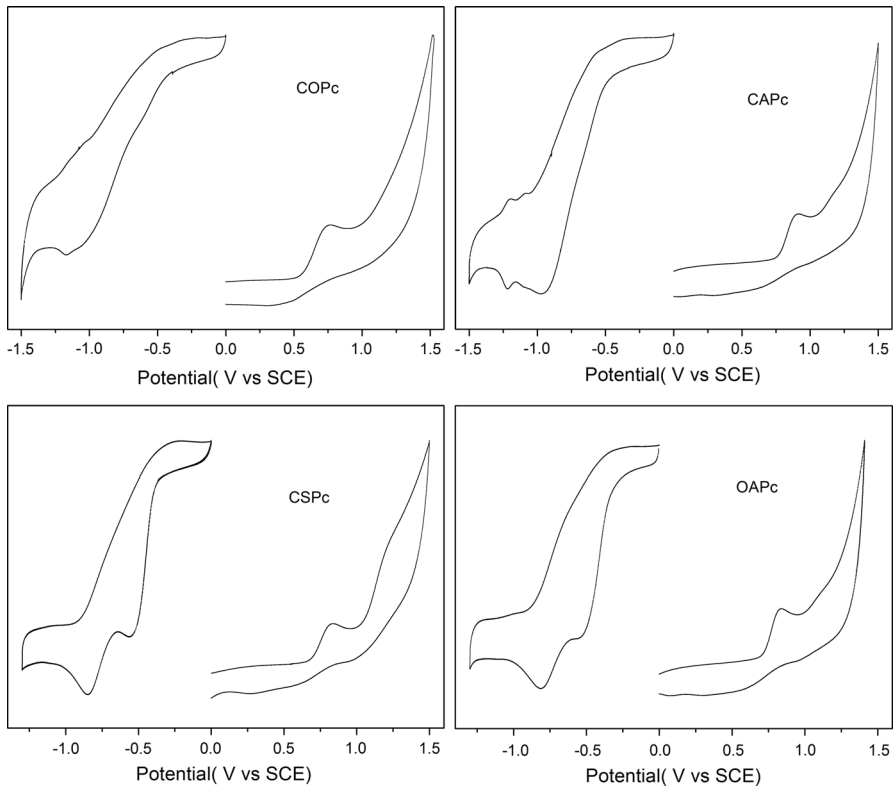


**Fig. 4** Cyclic voltammograms of phthalocyanines **COPc**, **CAPc**, **CSPc**, and **OAPc**

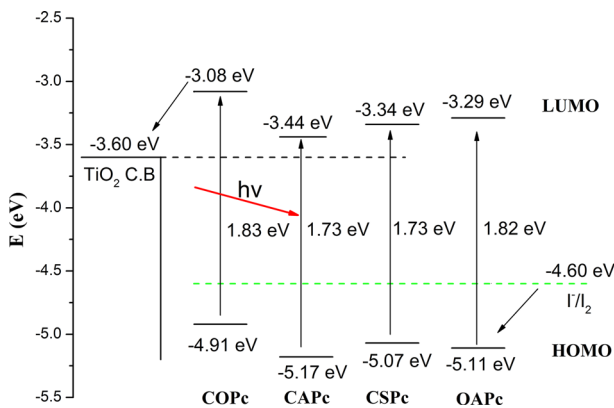


**Fig. 5** Energy-level diagrams for **COPc**, **CAPc**, **CSPc**, and **OAPc**

achieve efficient regeneration from the oxidized dyes, limiting further improvement of the energy conversion efficiency of DSSCs. The  $E_{\text{LUMO}}$  level and  $E_{\text{HOMO}}$  level of all the dyad dyes were found to fall in the range of  $-3.44$  to  $-3.08$  and  $-5.17$  V to

−4.91 V (versus SCE), respectively; the energy-level diagrams are shown in Fig. 5. The  $E_{\text{LUMO}}$  level was higher than the energy level for the conduction band (CB) of  $\text{TiO}_2$  (−3.6 eV versus vacuum), suggesting that electron injection from the excited dye to the CB of  $\text{TiO}_2$  is a thermodynamically favorable process. Besides, the  $E_{\text{HOMO}}$  level corresponding to the oxidation onset potentials of all the dyad dye sensitizers was more positive than the iodine/iodide redox potential (0.2 V versus SCE) [9, 13, 32], ensuring regeneration of the oxidized dyes by electron recapture from the redox electrolyte. In general, the dyad dyes containing  $\pi$ -conjugated moieties (**CAPc**, **CSPc**, and **OAPc**) possessed low  $E_{\text{HOMO}}$  (Fig. 5; Table 1) compared with their oxygen-linked counterpart (**COPc**). This low  $E_{\text{HOMO}}$  may suppress electron back-transfer from the CB of  $\text{TiO}_2$  to the oxidized dyes through facile regeneration of the oxidized dye, which will eventually increase  $V_{\text{OC}}$  due to accumulation of more electrons in the CB of  $\text{TiO}_2$ .

### Thermal degradation

The thermal stability of the synthesized dyad dyes was tested by thermogravimetric analysis under nitrogen atmosphere at heating rate of  $10\text{ }^\circ\text{C min}^{-1}$ ; the resulting TGA curves are shown in Fig. 6. Seoudi et al. [43] compared a series of unsubstituted metal phthalocyanines by thermogravimetric analysis, finding a first minor decomposition reaction at  $440\text{ }^\circ\text{C}$  and a major decomposition reaction at  $495\text{ }^\circ\text{C}$  for the phthalocyaninato zinc compounds, but when additional functional groups were introduced into the molecule, most of the substituted phthalocyanines were not as stable as their unsubstituted counterparts [38]. Recently, we reported the thermal behavior of a series of azo-coupled zinc phthalocyanine derivatives, whose TGA curves showed peaks at around  $400\text{ }^\circ\text{C}$  [30].

The TGA curve for the oxygen-linked dyad dye **COPc** shows three mass loss stages in the temperature range of  $150\text{--}700\text{ }^\circ\text{C}$ . The first stage onsets at  $214\text{ }^\circ\text{C}$  with mass loss of 41%, corresponding to loss of some carboxylic coumarin moieties,

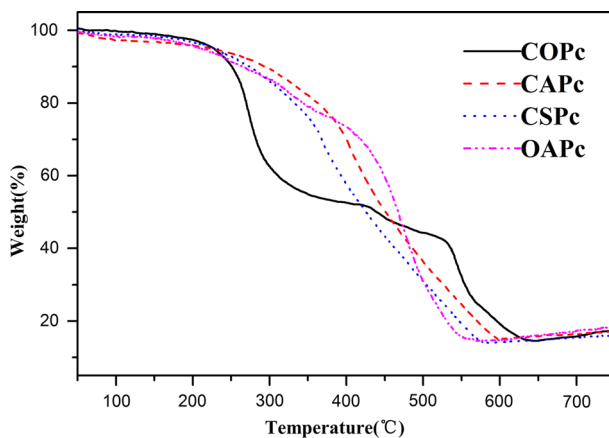


**Fig. 6** TGA curves of compounds **COPc**, **CAPc**, **CSPc**, and **OAPc**

while the other two stages that onset at 425 and 503 °C correspond to decomposition of phthalocyanine. The TGA curve of the azo-linked dye **CAPc** exhibits three different degradation stages. The weight loss of 12% observed between 200 and 309 °C corresponds to the theoretical content of the four carboxyl groups [44], and two major decomposition stages occurred at around 339 and 474 °C. The former decomposition stage begins with scission of N=N bonds [30, 33], while the latter maximum decomposition in the range of 437–474 °C is due to degradation of the phthalocyanine core itself. The TGA curve of the imino-linked dye **CSPc** exhibits degradation analogous to **CAPc**, consistent with the report of Mohamed et al. [45]. The asymmetric dyad dye **OAPc** showed slight decomposition with onset at around 205 °C, corresponding to loss of carboxyl group, and about 14% weight runaway ascribed to loss of azo moiety, with major decomposition in the range of 435–560 °C, possibly due to decomposition of the phthalocyanine core and 4-methylcoumarin substituent. Overall, it is clear that all the dyad sensitizers were stable up to 200 °C, indicating that all the dyad dyes are sufficiently thermally stable for rooftop applications of dye-sensitized solar cells.

### Photovoltaic performance

To evaluate the photovoltaic performance of compounds **COPc**, **CAPc**, **CSPc**, and **OAPc** as DSSC sensitizers, current–voltage curves for cells fabricated using TiO<sub>2</sub> electrodes sensitized with the dyad dyes were measured in ambient air under standard simulated AM1.5G illumination (100 mW cm<sup>-2</sup>) conditions (Fig. 7); the corresponding short-circuit currents ( $J_{SC}$ ), open-circuit potentials ( $V_{OC}$ ), fill factors (ff), and overall conversion efficiencies ( $\eta$ ) are presented in Table 2. The  $\eta$  values for the DSSCs based on these dyad dyes lay in the range of 0.9–2.4%. Among the dyes, the cell fabricated with the asymmetric dye **OAPc** exhibited high  $\eta$  (2.4%) with high  $J_{SC}$  of 8.1 mA cm<sup>-2</sup>,  $V_{OC}$  of 0.58 V, and fill factor (ff) of 0.53. Obviously, the  $\eta$  and  $J_{SC}$  values of cells sensitized using the  $\pi$ -conjugated dyad dyes

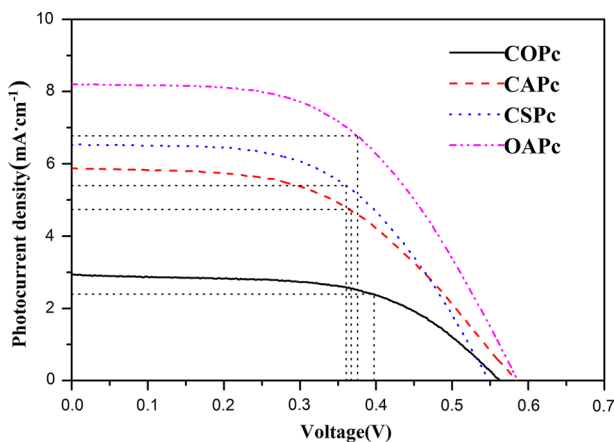


**Fig. 7** Photocurrent–voltage curves of DSSCs under simulated sun illumination

**Table 2** Photovoltaic characteristics of DSSCs sensitized by **COPc**, **CAPc**, **CSPc**, and **OAPc**

Compound	$J_{SC}$ (mA cm <sup>-2</sup> )	$V_{OC}$ (V)	ff	$\eta$ (%)
<b>COPc</b>	2.9	0.56	0.57	0.9
<b>CAPc</b>	5.8	0.58	0.51	1.7
<b>CSPc</b>	6.5	0.54	0.54	1.9
<b>OAPc</b>	8.1	0.58	0.53	2.4

**CAPc** and **CSPc** were slightly better than that using the dye **COPc** with oxygen bridge linkage. These results are ascribed to superior light-harvesting and effective electron transfer. Arguably, the efficiency of the cells using **CAPc** and **CSPc** is opposite to that expected based on their absorption spectra, which can be attributed to the aggregation behavior of **CAPc**. All the dyad dyes showed similar ff values, which is related to the fact that they contain both coumarin and phthalocyanine core. The comparatively high efficiency obtained when using the dye **OAPc** may originate from the following factors: (1) the presence of methylcoumarin as a steric hindrance moiety effectively suppresses dye aggregation, (2) the boarder and more efficient absorption spectrum, and (3) the asymmetric structure of the dye molecule that promotes electron transfer.

## Conclusions

A series of carboxyl coumarin–phthalocyanine dyad dyes conjugated by –O–, –N=N– or –N=C– bond in a single structure were designed, synthesized, and demonstrated as sensitizers in DSSCs. The influence of the linker on their absorption spectrum and electrochemical properties was revealed, and their photovoltaic parameters such as  $\eta$ ,  $J_{SC}$ , and  $V_{OC}$  studied. The absorption spectra demonstrate that the  $\pi$ -conjugated dyad dyes exhibited excellent absorption and photocurrent response across the whole visible-light region in the range of 400–800 nm due to reduction of the energy gap. The  $\pi$ -conjugated coumarin–phthalocyanine dyes **CAPc** and **CSPc** exhibited only moderate power conversion efficiency, mainly due to insufficient electron transfer of the symmetric coumarin-substituted phthalocyanine core. In contrast, the dyad dye **OAPc** exhibited improved asymmetric structure and efficiency of 2.4%. **CAPc** showed panchromatic response, but the **CAPc**-based DSSC showed low conversion efficiency. Further work to develop new asymmetric panchromatic dyes and improve their electron transfer is underway.

**Acknowledgements** The authors would like to acknowledge financial support from the Natural Science Foundation of Shanxi Province, China (Grant No. 2015011011) and the Research Project Supported by Shanxi Scholarship Council of China (Grant No. 2015-078).

## References

1. B. O'Regan, M. Grätzel, *Nature* **737**, 353 (1991)
2. M. Gratzel, *Nature* **338**, 414 (2001)

3. M.K. Nazeeruddin, F. De Angelis, S. Fantacci, A. Selloni, G. Viscardi, P. Liska, S. Ito, B. Takeru, M. Gratzel, *J. Am. Chem. Soc.* **16835**, 127 (2005)
4. M.J. Bosiak, M. Rakowiecki, A. Wolan, J. Szlachta, E. Stanek, D. Cycoń, K. Skupień, *Dyes Pigments* **79**, 121 (2015)
5. É. Torres, S. Sequeira, P. Parreira, P. Mendes, T. Silva, K. Lobato, M.J. Brites, *J. Photochem. Photobiol.* **1**, 310 (2015)
6. C. Zhong, J. Gao, Y. Cui, T. Li, L. Han, *J. Power Sources* **831**, 273 (2015)
7. S. Mathew, A. Yella, P. Gao, R. Humphry-Baker, B.F. Curchod, N. Ashari-Astani, I. Tavernelli, U. Rothlisberger, M.K. Nazeeruddin, M. Gratzel, *Nat. Chem.* **242**, 6 (2014)
8. Y. Xie, Y. Tang, W. Wu, Y. Wang, J. Liu, X. Li, H. Tian, W.H. Zhu, *J. Am. Chem. Soc.* **14055**, 137 (2015)
9. Z.-S. Huang, H. Meier, D. Cao, *J. Mater. Chem. C* **2404**, 4 (2016)
10. T. Ikeuchi, H. Nomoto, N. Masaki, M.J. Griffith, S. Mori, M. Kimura, *Chem. Commun.* **1941**, 50 (2014)
11. L. Giribabu, V.K. Singh, C.V. Kumar, Y. Soujanya, P.Y. Reddy, M.L. Kantam, *Sol. Energy* **1204**, 85 (2011)
12. L. Tejerina, M.V. Martinez-Diaz, M.K. Nazeeruddin, T. Torres, *Chem. Eur. J.* **4369**, 22 (2016)
13. G.S. Reddy, S. Ramkumar, A.M. Asiri, S. Anandan, *Spectrochim. Acta A* **531**, 145 (2015)
14. G.B. Bodedla, K.R. Justin Thomas, M.S. Fan, K.C. Ho, *J. Org. Chem.* **640**, 81 (2016)
15. K. Kakiage, Y. Aoyama, T. Yano, T. Otsuka, T. Kyomen, M. Unno, M. Hanaya, *Chem. Commun.* **6379**, 50 (2014)
16. B. Basheer, D. Mathew, B.K. George, C.P. Reghunadhan Nair, *Sol. Energy* **108**, 479 (2014)
17. Y. Ooyama, Y. Harima, *Eur. J. Org. Chem.* **2903**, 2009 (2009)
18. P. Kluson, M. Drobek, A. Kalaji, M. Karaskova, J. Rakusan, *Res. Chem. Intermed.* **103**, 35 (2009)
19. C.-P. Lee, R.Y.-Y. Lin, L.-Y. Lin, C.-T. Li, T.-C. Chu, S.-S. Sun, J.T. Lin, K.-C. Ho, *RSC Adv.* **23810**, 5 (2015)
20. S. Yamamoto, S. Mori, P. Wagner, A.J. Mozer, M. Kimura, *Isr. J. Chem.* **175**, 56 (2016)
21. M. Liang, J. Chen, *Chem. Soc. Rev.* **3453**, 42 (2013)
22. F. Liang, F. Shi, Y. Fu, L. Wang, X. Zhang, Z. Xie, Z. Su, *Sol. Energy Mater. Sol. Cells* **1803**, 94 (2010)
23. B. Ren, L. Zhu, G. Cui, Y. Sun, X. Zhang, F. Liang, Y. Liu, *Tetrahedron Lett.* **5953**, 54 (2013)
24. C.B. Kc, K. Stranius, P. D'Souza, N.K. Subbaiyan, H. Lemmetyinen, N.V. Tkachenko, F. D'Souza, *J. Phys. Chem. C* **763**, 117 (2013)
25. J. Wang, M. Li, D. Qi, W. Shen, R. He, S.H. Lin, *RSC Adv.* **53927**, 4 (2014)
26. A. Asli Esenpinar, M. Bulut, *Dyes Pigments* **249**, 76 (2008)
27. E. Dur, M. Bulut, *Polyhedron* **2689**, 29 (2010)
28. O. Soyer Can, E.N. Kaya, M. Durmuş, M. Bulut, *J. Photochem. Photobiol. A* **56**, 317 (2016)
29. A. Taştemel, B.Y. Karaca, M. Durmuş, M. Bulut, *J. Lumin.* **163**, 168 (2015)
30. M. Han, X. Zhang, X. Zhang, C. Liao, B. Zhu, Q. Li, *Polyhedron* **864**, 85 (2015)
31. L. Zhang, J.M. Cole, C. Dai, *ACS Appl. Mater. Interfaces* **7535**, 6 (2014)
32. B. Zhu, X. Zhang, M. Han, P. Deng, Q. Li, *J. Mol. Struct.* **61**, 1079 (2015)
33. H. Dinçalp, F. Toker, İ. Durucasu, N. Avcıbaşı, S. İcli, *Dyes Pigments* **11**, 75 (2007)
34. J. Yang, C. Ji, Y. Zhao, *Chin. J. Org. Chem.* **1740**, 28 (2008)
35. F. Chen, G. Liu, Y. Shi, P. Xi, J. Cheng, J. Hong, R. Shen, X. Yao, D. Bai, Z. Zeng, *Talanta* **139**, 124 (2014)
36. D.M. de Leeuw, M.M.J. Simenon, A.R. Brown, R.E.F. Einerhand, *Synth. Met.* **53**, 87 (1997)
37. Y. Liu, Q. Yang, D. Hao, W. Zhang, *Aust. J. Chem.* **1390**, 65 (2012)
38. F. Ghani, J. Kristen, H. Riegler, *J. Chem. Eng. Data* **439**, 57 (2012)
39. Y. Liu, H. Lin, X. Li, J. Li, H. Nan, *Inorg. Chem. Commun.* **187**, 13 (2010)
40. R.Z.U. Kobak, M.U. Ari, A. Tekin, A. Gül, *Chem. Phys.* **91**, 448 (2015)
41. Z. Ning, Y. Fu, H. Tian, *Energy Environ. Sci.* **1170**, 3 (2010)
42. M. Ikiz, E. İspir, E. Aytar, E. Aytar, M. Ulusoy, S. Karabuga, M. Aslantas, O. Celik, *New J. Chem.* **8204**, 39 (2015)
43. R. Seoudi, G.S. El-Bahy, Z.A. El Sayed, *J. Mol. Struct.* **119**, 753 (2005)
44. M. Sreenivasu, A. Suzuki, M. Adachi, C.V. Kumar, B. Srikanth, S. Rajendar, D. Rambabu, R.S. Kumar, P. Malleshm, N.V. Rao, M.S. Kumar, P.Y. Reddy, *Chem. Eur. J.* **14074**, 20 (2014)
45. G.G. Mohamed, M.M. Omar, A.M. Hindy, *Spectrochim. Acta A* **1140**, 62 (2005)